05,13

Peculiarities of the formation of band gaps in mul-timode regime of spin waves propagation in mag-nonic crystals

© A.A. Martyshkin[1], E.N. Beginin[1], S.E. Sheshukova[1], Yu.P. Sharaevsky[1], S.A. Nikitov[1,2], A.V. Sadovnikov[1,2]

[1] Saratov National Research State University, Saratov, Russia
[2] Kotelnikov Institute of Radio Engineering and Electronics, Russian Academy of Sciences, Moscow, Russia
E-mail: aamartyshkin@gmail.com

Received April 29, 2022
Revised April 29, 2022
Accepted May 12, 2022

The dynamics of spin waves during their multimode propagation in a magnonic crystal, which is an irregular narrow ferrite waveguide with periodic boundary modulation, has been studied by the method of Mandelstam–Brillouin spectroscopy. The transformation of the mode composition of spin waves propagating in an irregular ferrite waveguide is shown. The space-time dynamics of spin waves and the characteristics of the band gaps of a magnonic crystal are experimentally studied, and the possibility of controlling the frequency-selective properties of such a structure is shown. By excitation of a superposition of even or odd width modes of the ferrite microstructure, it becomes possible to control the position of the band gaps of a magnonic crystal. The results of the experiment agree with the results of micromagnetic modeling of the propagation and transformation of the spectrum of spin waves propagating in a ferromagnetic periodic structure.

Keywords: spin waves, magnonics, magnonic crystal, micromagnetic modeling.

DOI: 10.21883/PSS.2022.09.54164.17HH

1. Introduction

Currently, spin waves propagating in planar ferromagnetic structures of various dimensions (one-dimensional (1D) and two-dimensional (2D)) with periodic spatial modulation of parameters are being actively studied [1]. Periodic structures can be created in various ways, for example: by spatial variation of the magnetic properties of materials (for example, saturation magnetization) [2], by changing the thickness or width of planar waveguide magnetic structures [3–5], by creating two-dimensional magnetic gratings [6], spatial modulation of static magnetic fields [6], etc. Such periodic structures, called magnonic crystals (MC) [1,3], are characterized by the presence of band gaps at frequencies where the Bragg condition $k_{\mathrm{B}} = n\pi/L$ is satisfied (where L is the structure period, k_{B} is the Bragg wave number, n is the band number). The band gap parameters (depth, frequency width) depend, in particular, on the relative modulation depth of the spatial parameters $\xi = \Delta w/w_0$, where Δw is variation, w_0 is the average value of the parameter, respectively.

MCs can be used as an element base for the development of various functional devices for signal processing in the microwave range of radio waves: resonators, couplers, delay lines, filters, phase shifters, etc. Theoretically and experimentally, 1D-MC (variation of medium parameters or geometrical dimensions along one of the directions) based on constant-width waveguides with characteristic transverse dimensions of $2-3$ mm and a low modulation value $\xi < 0.1$ are the most well studied. In such MCs, wave propagation can be considered single-mode, and the scattering of waves by heterogeneities occurs without excitation of higher modes. For the theoretical study of such MCs, methods based on the single-wave approximation are widely used: the coupled wave method [7], the transfer matrix method [4], the plane wave method [8], etc.

The miniaturization of the element base and the creation of integrated circuits for information processing systems necessitates a transition to the region of micron and sub-micron spatial scales of MC with a simultaneous decrease in the length of propagating waves. In this region of spatial scales, waveguides based on permalloy films are the main type of waveguide structure for creating 1D-MC. MCs based on waveguides with a periodic width change have been experimentally and theoretically studied in a number of articles [4,9]. For this type of MCs, the magnitude ξ determines the relative modulation depth of the waveguide width. At low modulation $\xi < 0.1$, one can also use the single-wave approximation to analyze such structures. However, even in this case, the excitation and propagation of waves in transversely limited MCs is essentially multimode, the spectrum of transverse wave numbers is quantized, and branches corresponding to the so-called width modes appear in the dispersion characteristics of $\omega(k)$ waves. As the waveguide width w_0 decreases and the frequency ω is fixed, the intermode distance Δk in terms of wave numbers between the branches increases. In regular waveguides, these modes propagate independently; however, in the waveguides with width modulation, an increase in the modulation depth ξ can lead to coupling of the width modes scattered at heterogeneous waveguide boundaries. For large modulation ξ ($\xi > 0.1$), it is necessary to take into account the intermode interaction of propagating waves in the formation of band gaps [10].

Thin films of yttrium iron garnet (YIG), compared to permalloy, have significantly lower dissipation parameters and are widely used to create MC and controllable devices for spintronics and magnonics [1,4,8]. With a decrease in the transverse dimensions of regular waveguides based on YIG to hundreds of microns, the nature of wave propagation also has an essentially multimode character. It is of interest to study the features of formation of band gaps in MCs based on YIG waveguides with the periodic modulation of the width and spatial distribution of the intensity of spin-wave excitations at different frequencies. As a rule, magnon crystals based on waveguides are a combination of regular and periodic waveguide structures with different spectra of natural waves, and the excitation of waves is carried out by microstrip antennas located in a regular waveguide.

In the present article, we study an irregular YIG waveguide, which consists of two sections connected by a YIG waveguide with a linearly varying width. The first section is a wide waveguide, in the region of which spin waves are excited by a microstrip antenna. The second section is MC based on a narrow waveguide with periodic width modulation. A waveguide with a variable width acts as a matching element [11] and can be used to control the mode composition of spin waves propagating in the MC region [12,13].

Experimental measurement of the spatial distribution of wave amplitudes can be carried out by various methods, for example, by microwave probes. However, as the geometric dimensions of the waveguides decrease (less than 500 μm), the spatial resolution of the probe methods becomes insufficient. At present, to study the spatial and temporal characteristics of waves in waveguides of micron and submicron sizes, the method of Brillouin light scattering on magnetic excitations in ferromagnetic structures (BLS) [14] is widely used. In this article, we present the results of the study of the formation of band gaps and multimode propagation of magnetostatic waves in a 1D-MC in various frequency domains by the BLS method.

2. Experimental and numerical study

To create MC, we used a single-crystal YIG film [$Y_3Fe_2(FeO_4)_3(111)$] with a thickness of $d = 10\,\mu$m, saturation magnetization $4\pi M_0 = 1350$ G, grown on a gallium-gadolinium base 500 μm thick. An irregular waveguide of magnetostatic waves was created on the surface of the YIG film by laser scribing [15] by connecting two regular waveguides with a width of 2000 μm and $w_0 = 353\,\mu$m through a section waveguide with a linear width variation

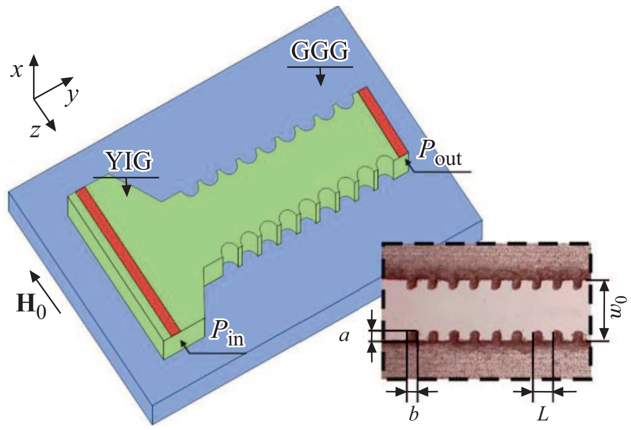

Figure 1. An irregular waveguide with a periodically changing width (1D MC), in the inset — a photograph of a fragment of the structure with dimensions $a = 60\,\mu$m, $b = 60\,\mu$m, $L = 122\,\mu$m, $w_0 = 353\,\mu$m.

(Fig. 1). In a narrow waveguide, a 1D MC was created in a similar way with a periodic sequence of rectangular cutouts at its edges and geometric dimensions shown in the inset to Fig. 1. The total length of the irregular waveguide was 6 mm, the length of the narrow waveguide with MC — 5 mm. To excite magnetostatic waves (MSWs), microstrip antennas of spin waves with a width of 30 μm and a length of 3 mm were used. The input antenna was located in the wide part of the irregular waveguide at a distance of 1.5 mm from the plane corresponding to the beginning of the periodic structure in the narrow waveguide. The output antenna was located in the narrow part of the waveguide at a distance of $h = 5$ mm from the input antenna. The waveguide with MC was placed in an external uniform magnetic field $H_0 = 440$ Oe, oriented in the waveguide plane along the antenna axis. Surface MSWs were excited in the irregular waveguide with MC.

Elements of the MC scattering matrix (S-parameters) in the microwave range of radio waves were measured by a vector network analyzer (VNA). Fig. 2 shows the results of measuring the S-parameters (black curve) of MC at the input power of the microwave signal $P_{in} = -30$ dB to eliminate the effect of three-magnon decay processes of spin waves. The dispersion characteristic of MSW (Fig. 2, a) was found based on the measured value of the phase incursion $\varphi(f)$ of MSW between the microstrip antennas using the relation $k(f) = \varphi(f)/h$.

Micromagnetic modeling was carried out in MuMax3 software [16] based on the numerical solution of the Landau–Lifshitz–Gilbert equation:

$$\frac{\partial \mathbf{M}}{\partial t} = -\gamma[\mathbf{H}_{\rm eff} \times \mathbf{M}] + \frac{\alpha}{M_s}\left[\mathbf{M} \times \frac{\partial \mathbf{M}}{\partial t}\right],$$

which describes the precession of the magnetic moment M in the effective magnetic field $H_{\rm eff} = H_0 + H_{\rm demag} + H_{\rm ex} + H_a$, where H_0 is an external magnetic field,

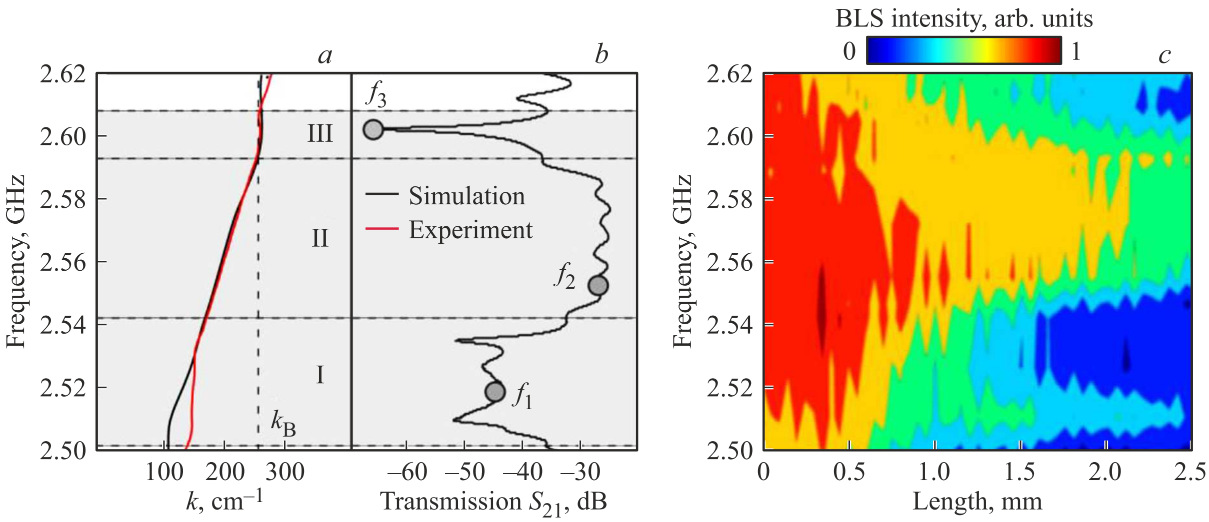

Figure 2. Dispersion characteristics of MSW (a) constructed based on experimental data (black curve) and using numerical simulation (red curve). The frequency transmission factor is S_{21} (b). The dots mark the characteristic frequencies where measurements were made $f_1 = 2.519$, $f_2 = 2.55$, $f_3 = 2.608$ GHz. c is spatial-frequency distribution of the $I(y, f)$ MSW intensity in MC.

H_{demag} is a demagnetizing field, H_{ex} is an exchange field, H_a is an anisotropy field. In this case, the YIG anisotropy field was not taken into account. To reduce the signal reflections from the calculated area boundaries the regions with geometrically increasing decay coefficient $\alpha = 10^{-5}$–1 at the waveguide structure boundaries were introduced [17]. To create the structure, thin YIG films with saturation magnetization $4\pi M_s = 1750$ G were used as a magnetic microwave guide. Dimensionless dissipation parameter was equal to $\alpha = 10^{-5}$, while the exchange hardness $A_{\text{ex}} = 3 \cdot 10^{-7}$ erg/cm. The structure under study can be represented as a waveguide system, which is a magnetic strip modulated in width, forming a spin-wave channel placed in an external uniform magnetic field $H_0 = 440$ Oe directed along the x axis (Fig. 1, a).

The values of dynamic magnetization $m_z(x, y, t)$ were calculated, while the input signal of the alternating magnetic field created by the microstrip with current was set as $b_z(t) = b_0 \sin c(2\pi f_c t)$, where $f_c = 10$ GHz, $b_0 = 10$ mOe. Dynamic magnetization was recorded with a pitch of $\delta t = 75$ fs during the time $T = 300$ ns. Further, using the double Fourier transform, the MSW dispersion characteristics (Fig. 2, a (red curve)) were constructed, which qualitatively coincide with the experimental results.

Fig. 2, b shows the results of measuring the modulus of the frequency transmission factor $S_{21}(f)$.

Dependence $S_{21}(f)$ can be divided into three characteristic frequency regions with different MSW attenuation levels. Region I with a high attenuation level — 50 dB is located near the beginning of the MSW spectrum with wave numbers $k \sim 100\,\text{cm}^{-1}$. Region III with central frequency $f_3 = 2.608$ GHz, attenuation level — 60 dB corresponds to MSW with wave numbers $k \sim 240\,\text{cm}^{-1}$. Regions I and III are separated by region II, where MSWs propagate with relatively small attenuation ($S_{21} \simeq 30$ dB). It follows from the experimentally measured dispersion characteristic of MC that region III corresponds to MSWs with wave numbers close to the wave number k_B of the first Bragg band gap $k \sim k_B = \pi/L = 257\,\text{cm}^{-1}$.

The mechanism for the appearance of the MSW rejection zone in region I is due to the multimode composition of the propagating MSW. The BLS method was used to study the spatial distribution of the MSW intensity in MC at different frequencies when the structure was excited by pulsed microwave signals with duration $\tau = 200$ ns, repetition period $T_i = 1.5\,\mu$s, of different power. Scanning of the investigated irregular waveguide was carried out with different spatial resolution $\Delta y \Delta z = 0.05 \times 0.03$ mm. The intensity of scattered light on spin waves is determined by the expression $I(y, z, t) \propto |m(y, z, t)|^2$, where $m(y, z, t)$ is MSW amplitude.

Fig. 2, c shows the spatial-frequency distribution of the integrated intensity

$$I(f, y) = \int_0^{T_i} \int_0^{w_0} I(f, y, z, t)dz\,dt/I_0(f),$$

where $I_0(f)$ is integrated intensity measured in the section $y_{\text{mc}} = 0$ (mc is magnonic crystal) at a given frequency f. Note that the beginning of MC in a narrow waveguide corresponds to the coordinate $y_{\text{ms}} = 0.25$ mm. In Fig. 2, c, two frequency regions are observed with a strong spatial attenuation of MSW, and the position of these regions on the frequency axis corresponds to regions I, III in Fig. 2, b. Formation of band gaps in this case occurs at a distance of the order of 1 mm from the beginning of MC, at which about 10 periods of the structure fit. Thus, there is a spatial formation of band gaps due to MSW scattering at the periodic edges of the waveguide.

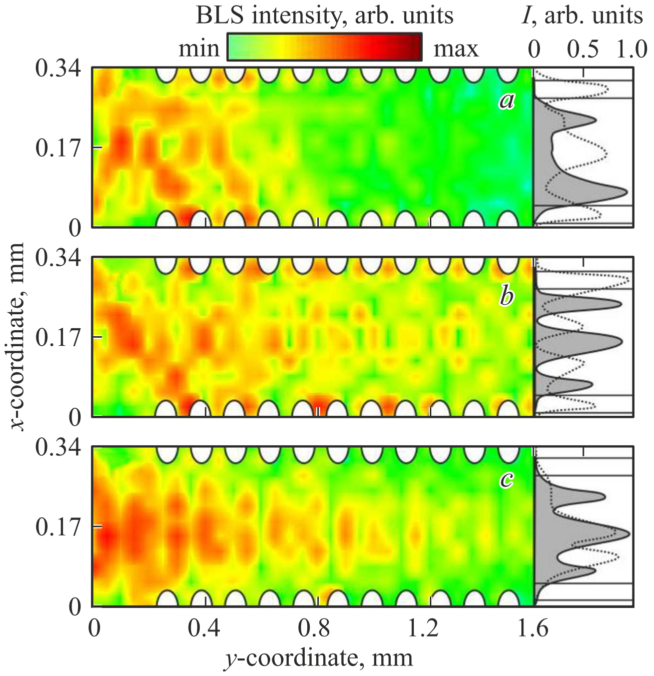

Figure 3. Spatial distribution of $I(y, z)$ of MSWs in MC at different frequencies of the input microwave signal: f_1 (a), f_2 (b), f_3 (c) and transverse distributions of $I(z)$ in the wide ($y = 0.7$ mm, dotted line) and the narrow part of the waveguide (0.76 mm, solid line).

Spatial distribution of spin waves in MC is characterized by the integral intensity

$$I(y, z) = \int_0^T I(y, z, t)dt.$$

The $I(y, z)$ distribution showed that at all frequencies in the regular part of the narrow waveguide before the beginning of MC ($y < y_{ms}$), MSW modes propagate with a transverse distribution of amplitudes according to the law $\sin(n\pi z/w_0)$, $n = 1, 3, \ldots$. The modes with $n = 1$ and $n = 3$ make the main contribution to the formation of the pattern of the spatial distribution of the spin wave intensity. In the considered waveguide, the multimode mode of excitation and propagation of MSWs in the MC [18] is implemented.

Fig. 3 shows the spatial distributions of the integrated MSW intensity I(y, z) measured at frequencies f_1, f_2, f_3. The same figure (right column) shows the transverse intensity distributions in the wide and narrow parts of the waveguide (in the section $y = 0.7$ mm and $y = 0.76$ mm, respectively).

At all frequencies in the MC region, a regular spatial pattern of the MSW intensity distribution is formed due to the superposition of the modes incident and scattered at the MC edges with different mode indices n. The intensity distribution is practically symmetrical with respect to the longitudinal axis of the MC, i.e., n takes odd values. It should be noted that, by changing the width of the waveguide structure, it becomes possible to control the mode composition of the propagating MSWs: violation of the axial symmetry of the structure leads to the formation of even width modes, while if the axial symmetry is preserved when the film waveguide width is changed, the mode composition of the propagating MSWs does not change.

To estimate the intermode interaction in the magnon-crystalline microwave guide under consideration, we used the model of junction of two semi-infinite waveguide sections of ferrite microwave guides of different widths (w_1 and w_2). The problem of spin wave diffraction at the junction of two semi-infinite waveguides is considered in the electrodynamic approximation in [19]. The dispersion of the first and third width modes for ferrite microwave guides with the width $w_1 = 353$ mkm and $w_2 = 233$ mkm is shown in Fig. 4, where the intensity distribution profiles of spin wave across microwave guides are schematically shown. When changing the waveguide width modulation parameter$\delta = \frac{w_1 - w_2}{w_1}$ the degree of coupling of the first waveguide mode w_1 wide with the first

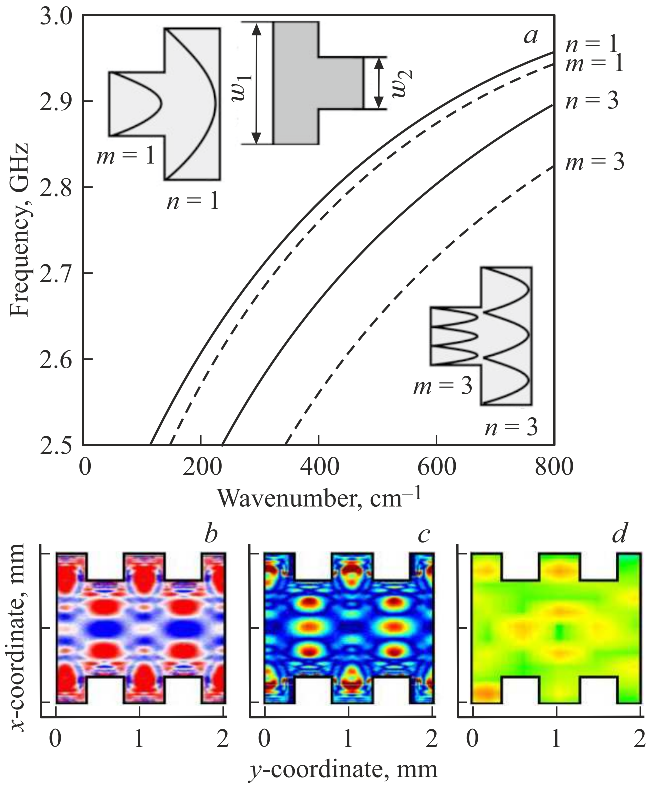

Figure 4. Dispersions of the first and third width modes for ferrite microwave guides with the width $w_1 = 353\,\mu$m and $w_2 = 233\,\mu$m (a). The result of calculating dynamic magnetization at a distance of 1.2 mm from the input antenna in the form of maps of the spatial distribution of the magnetization component m_z (b), intensity $I(y, z)$ (c) and an experimental map of the integrated intensity distribution $I(y, z)$ MSV (d).

three microwaveguide modes w_2 wide will change. In article [20] it is shown that the band gap in periodic structures in the approximation of small index $\delta \ll 1$ is proportional to the modulation index of the periodicity parameter. Consequently, an increase in the modulation index leads to an increase in the band gap. However, to observe band gaps for waves with different indices, it is necessary that the waveguides have a sufficiently small width. Then the spectrum of eigenmodes will be sufficiently discharged, and the Bragg reflection conditions for each eigenmode will be satisfied at very different frequencies. For any value of the modulation index, the effective coupling decreases with an increase in the mode index n. With an increase in the modulation index in the case of excitation of a fundamental mode in a section with a width of w_1, a decrease in coupling with the first mode and an increase in coupling with the second and third modes in a section with a width of w_2 will be observed. In the experimentally studied waveguide, the width modulation index has a value of the order of $\delta = 0.33$, and a fairly effective intermode coupling of magnetostatic waves is observed. The propagating higher modes are also scattered at the junctions of waveguides of different cross sections, forming band gaps in the dispersion branches of the corresponding modes. To prove this effect, micromagnetic simulation was carried out, in which the signal was excited at the left boundary of the structure with a spatial profile corresponding to the first width mode of the microwaveguide with a width of w_1. Fig. 4, *b, c* shows the result of calculating dynamic magnetization at a distance of 1.2 mm from the input antenna in the form of maps of the spatial distribution of the magnetization component m_z and intensity $I = \sqrt{m_z^2 + m_y^2}$. For comparison with experimental measurements, Fig. 4 *d* shows the region of the MSW integrated intensity distribution map $I(y, z)$. The number of maxima in the micromagnetic and experimental studies in the narrow section coincides, which confirms the intermode interaction observed in the experiment.

3. Conclusion

Using the magnetic material Brillouin spectroscopy method, we studied the features of multimode MSW propagation in an irregular YIG waveguide with a periodically modulated width, formed from a YIG film by laser scribing. It is shown that, by changing the width of the waveguide structure, it becomes possible to control the mode composition of the propagating MSWs: violation of the axial symmetry of the structure leads to the formation of even width modes, while if the axial symmetry is preserved when the film waveguide width is changed, the mode composition of the propagating MSWs does not change. The existence of band gaps was shown on the experimentally obtained spatial-frequency distributions of intensity. The band gap in the low-frequency region is formed due to the intermode interaction of MSWs and reflections from periodic heterogeneities at the boundaries. The high-frequency band corresponds to the Bragg band gap of a magnonic crystal with weak periodic modulation of the boundary. Propagation of a microwave pulse in 1D MC at frequencies between band gaps was accompanied by the excitation of localized MSW modes at the edges of the structure. These effects must be taken into account when constructing mathematical models of this type of 1D-MC and fabricating frequency-selective devices based on them.

Funding

The study was performed with the support of the Ministry of Education and Science of Russia under the Government Task (project No. FSRR-2020-0005).

Conflict of interest

The authors declare that they have no conflict of interest.

References

[1] A.V. Sadovnikov, A.A. Grachev, S.E. Sheshukova, S.A. Nikitov, J.-Y. Duquesne, M. Marangolo. J. Phys.: Condens. Matter **33**, 413001 (2021)
[2] B. Obry, P. Pirro, Th. Bracher, A. Chumak, J. Osten, F. Ciubotaru. Appl. Phys. Lett. **102**, 202403 (2013).
[3] S.A. Nikitov, A.R. Safin, D.V. Kalyabin, A.V. Sadovnikov, E.N. Beginin, M.V. Logunov, M.A. Morozova, S.A. Odintsov, S.A. Osokin, A.Yu. Sharaevskaya, Yu.P. Sharaevsky, A.I. Kirilyuk. UFN, **190**, 1009 (2020) (in Russian).
[4] A.V. Chumak, A.A. Serga, M.P. Kostylev, R.L. Stamps, H. Schultheiss, K. Vogt, S.J. Hermsdoerfer, B. Laegel, P.A. Beck, B. Hillebrands. Appl. Phys. Lett. **95**, 262508 (2009).
[5] M. Arikan, Y. Au, G. Vasile, S. Ingvarsson, V.V. Kruglyak. J. Phys. D **46**, 135003 (2013).
[6] V.V. Kruglyak, P.S. Keatley, A. Neudert, R.J. Hicken, J.R. Childress, J.A. Katine. Phys. Rev. Lett. **104**, 027201 (2010).
[7] M.A. Morozova, S.A. Nikitov, Yu.P. Sharaevskii, S.E. Sheshukova. Acta Phys. Polon. A **121**, 1173 (2012).
[8] M. Krawczyk, H. Puszkarski. Phys. Rev. B **77**, 054437 (2008).
[9] F. Ciubotaru, A.V. Chumak, N.Yu. Grigoryeva, A.A. Serga, B. Hillebrands. J. Phys. D **45**, 255002 (2012).
[10] K.-S. Lee, D.-S. Han, S.-K. Kim. Phys. Rev. Lett. **102**, 127202 (2009).
[11] V.E. Demidov, M.P. Kostylev, K. Rott, J. Münchenberger, G. Reiss, S.O. Demokritov. Appl. Phys. Lett. **99**, 082507 (2011).
[12] E.N. Beginin, A.V. Sadovnikov, Yu.P. Sharaevsky, S.A. Nikitov. Solid State Phenomena **215**, 389 (2014).
[13] E.N. Beginin, A.V. Sadovnikov, Yu.P. Sharaevsky, S.A. Nikitov. Izv. RAN. Ser. fiz. **77**, 1735 (2013) (in Russian).
[14] V.E. Demidov, J. Jersch, S.O. Demokritov, K. Rott, P. Krzysteczko, G. Reiss. Phys. Rev. B **79**, 054417 (2009).

[15] E.N. Beginin, A.V. Sadovnikov, Yu.P. Sharaevsky, S.A. Nikitov. Solid State Phenomena **215**, 389 (2014).
[16] A. Vansteenkiste, J. Leliaert, M. Dvornik, M. Helsen, F. Garcia-Sanchez, B. Van Waeyenberge. AIP Advances **4**, 107133 (2014).
[17] G. Venkat, H. Fangohr. JMMM **450**, 34 (2018).
[18] S.O. Demokritov, B. Hillebrands, A.N. Slavin. Phys. Rep. **348**, 441 (2001).
[19] L.A. Vainshtein. Elektromagnitnye volny. Radio i svyaz, M. (1988). 440 s. (in Russian).
[20] A.D. Grigoriev. Elektrodinamika i mikrovolnovaya tekhnika. 2-e izd. Lan, SPb (2007). 704 s. (in Russian).